J|A|C|S ARTICLES

Published on Web 11/06/2009

Au Growth on Semiconductor Nanorods: Photoinduced versus Thermal Growth Mechanisms

Gabi Menagen,[†,‡] Janet E. Macdonald,[†,‡] Yossi Shemesh,[†,‡] Inna Popov,[‡] and Uri Banin*[,†,‡]

Institute of Chemistry and The Center for Nanoscience and Nanotechnology, The Hebrew University of Jerusalem, Jerusalem 91904, Israel

Received September 13, 2009; E-mail: banin@chem.ch.huji.ac.il

Abstract: Gold growth on CdS nanorods and on seeded CdSe/CdS nanorods with and without illumination at different temperatures was studied. Two competing mechanisms were identified: thermal and light-induced growth. The thermal mechanism leads to growth of small gold particles at defects along the rod body and can be suppressed at lower temperatures. This control is attributed to a phase transition of the alkyl chains of the surface amine ligands to a static phase at lower temperatures, blocking the Au precursor's access to the nanorod surfaces. While a long-chain (C18) amine shows effective blocking at 293 K, a shorter chain (C12) amine shows the same result only at 273 K; however, in the case of a bulky trialkylamine, defect growth was observed even at 273 K. Light-induced growth leads to selective deposition of gold on one end of the rods. The tip was shown to grow on sulfur-rich facets of the nanorod, producing end-on and angled tip orientations. Growth under illumination with decreased temperature provides a highly selective synthesis of hybrid semiconductor nanorods with a single gold tip. Such anisotropic semiconductor−metal hybrids are of interest for self-assembly and photocatalysis and as building blocks in optoelectronic devices.

Introduction

Hybrid metal−semiconductor nanoparticles (NPs) combine, on one nanoparticle, disparate materials that enhance the functionality of the system. The preparation of hybrid metal−semiconductor NPs presents new synthetic challenges in combining the two disparate material systems onto one NP in a controlled manner. Metal tips have been grown on one or both sides of nanorods, providing an anchor point for self-assembly and for electrical connections.[1−6] The metal−semiconductor interface serves as a model system for such contacts at the nanoscale and also exhibits light-induced charge separation.[7−10] This latter feature has important consequences for solar energy harvesting, in the use of such systems either as photocatalysts[11−15] or as building blocks in solar cells.

Two main routes have typically been used for growth of such hybrids, with the semiconductor NP serving as a template for the metal growth. The first route is via a solution reaction of a metal salt with the semiconductor NPs. Specific ligands were employed to stabilize the nanorods and also to play a role in the metal reduction.[1,2,16,17] A high-temperature growth of Pt and Co on II−VI semiconductor nanorods was also reported.[18−20] The second route employs light-induced growth of the metal onto the semiconductor NP.[7,21−23] A model system for these two processes is provided by Au growth onto CdS nanorods or

[†] Institute of Chemistry.
[‡] The Center for Nanoscience and Nanotechnology.

(1) Mokari, T.; Rothenberg, E.; Popov, I.; Costi, R.; Banin, U. *Science* **2004**, *304*, 1787–1790.
(2) Mokari, T.; Sztrum, C. G.; Salant, A.; Rabani, E.; Banin, U. *Nat. Mater.* **2005**, *4*, 855–863.
(3) Zhao, N.; Liu, K.; Greener, J.; Nie, Z. H.; Kumacheva, E. *Nano Lett.* **2009**, *9*, 3077–3081.
(4) Salant, A.; Amitay-Sadovsky, E.; Banin, U. *J. Am. Chem. Soc.* **2006**, *128*, 10006–10007.
(5) Figuerola, A.; Franchini, I. R.; Fiore, A.; Mastria, R.; Falqui, A.; Bertoni, G.; Bals, S.; Van Tendeloo, G.; Kudera, S.; Cingolani, R.; Manna, L. *Adv. Mater.* **2009**, *21*, 550–554.
(6) Sheldon, M. T.; Trudeau, P.-E.; Mokari, T.; Wang, L.-W.; Alivisatos, A. P. *Nano Lett.* Published ASAP online Aug 19, 2009, http://dx.doi.org/10.1021/nl902186v.
(7) Wood, A.; Giersig, M.; Mulvaney, P. *J. Phys. Chem. B* **2001**, *105*, 8810–8815.
(8) Subramanian, V.; Wolf, E. E.; Kamat, P. V. *J. Am. Chem. Soc.* **2004**, *126*, 4943–4950.
(9) Chen, W. T.; Yang, T. T.; Hsu, Y. J. *Chem. Mater.* **2008**, *20*, 7204–7206.
(10) Costi, R.; Cohen, G.; Salant, A.; Rabani, E.; Banin, U. *Nano Lett.* **2009**, *9*, 2031–2039.
(11) Ung, T.; Liz-Marzan, L. M.; Mulvaney, P. *J. Phys. Chem. B* **1999**, *103*, 6770–6773.
(12) Cozzoli, P. D.; Comparelli, R.; Fanizza, E.; Curri, M. L.; Agostiano, A.; Laub, D. *J. Am. Chem. Soc.* **2004**, *126*, 3868–3879.
(13) Hirakawa, T.; Kamat, P. V. *J. Am. Chem. Soc.* **2005**, *127*, 3928–3934.
(14) Elmalem, E.; Saunders, A. E.; Costi, R.; Salant, A.; Banin, U. *Adv. Mater.* **2008**, *20*, 4312–4317.
(15) Costi, R.; Saunders, A. E.; Elmalem, E.; Salant, A.; Banin, U. *Nano Lett.* **2008**, *8*, 637–641.
(16) Saunders, A. E.; Popov, I.; Banin, U. *J. Phys. Chem. B* **2006**, *110*, 25421–25429.
(17) Menagen, G.; Mocatta, D.; Salant, A.; Popov, I.; Dorfs, D.; Banin, U. *Chem. Mater.* **2008**, *20*, 6900–6902.
(18) Habas, S. E.; Yang, P. D.; Mokari, T. *J. Am. Chem. Soc.* **2008**, *130*, 3294–3295.
(19) Maynadie, J.; Salant, A.; Falqui, A.; Respaud, M.; Shaviv, E.; Banin, U.; Soulantica, K.; Chaudret, B. *Angew. Chem., Int. Ed.* **2009**, *48*, 1814–1817.
(20) Deka, S.; Falqui, A.; Bertoni, G.; Sangregorio, C.; Poneti, G.; Morello, G.; De Giorgi, M.; Giannini, C.; Cingolani, R.; Manna, L.; Cozzoli, P. D. *J. Am. Chem. Soc.* **2009**, *131*, 12817–12828.
(21) Pacholski, C.; Kornowski, A.; Weller, H. *Angew. Chem., Int. Ed.* **2004**, *43*, 4774–4777.
(22) Dukovic, G.; Merkle, M. G.; Nelson, J. H.; Hughes, S. M.; Alivisatos, A. P. *Adv. Mater.* **2008**, *20*, 4306–4311.

10.1021/ja9077733 CCC: $40.75

onto related heterostructured seeded nanorods.[16,17] Previously in our laboratory, a simple solution reaction route in ambient light was studied, which led to Au growth on defect sites along the CdS nanorod surface, while long reaction times yielded the additional growth of a large metal tip on one end.[16] The same reaction for seeded CdSe/CdS nanorods with a thin CdS shell yielded instead selective growth of a larger Au dot onto the seed location, along with defect growth in other locations. This was assigned to electrochemical Ostwald ripening[24] of the Au onto the location next to the seed, which is known to localize electrons in this system. Indeed, growth of Au on seeded CdSe/CdS nanorods with a thick shell, or onto ZnSe/CdS seeded nanorods, resulted in only defect growth, consistent with the electronic structures of these types of particles that do not provide electron localization.[17,25] Recently, Sönnichsen and coworkers studied the growth of Au onto seeded CdSe/CdS nanorods, utilizing a light-induced reaction.[26] However, this reaction still yielded significant defect growth. To date, there is little understanding of the interplay between thermal and light-induced growth in these systems. Moreover, a facile solution route to hybrid NPs of CdS nanorods with only tip growth has not been reported. This will allow future characterization and understanding of the structure−property relationships of these hybrid NPs.

Here we present the further control of Au growth onto such structures and provide a description of the underlying mechanisms. The effects of light-induced growth versus growth in the dark is demonstrated, where the former leads to growth of a large Au tip on one end of the rod. We also investigate the effect of reaction temperature and find that defect growth is suppressed at lower temperatures. The prevention of surface defect growth is attributed to a phase transition in the alkyl chains of the ligand shell,[27,28] as supported by a study of the dependence of the growth on the surface ligands. The findings enrich the understanding of the growth mechanisms in hybrid metal−semiconductor NPs and also provide a facile route to well-controlled asymmetric hybrid systems with a single exposed Au tip on one end.

Experimental Section

To prepare CdS or seeded CdSe/CdS nanorods, the seeded growth method of Manna et al. was employed.[29] Briefly, a precursor solution of either CdS or CdSe seed dots and sulfur was rapidly injected into a solution of the cadmium precursor dissolved in a mixture of *n*-trioctylphosphineoxide (TOPO), *n*-trioctylphosphine (TOP), and phosphonic acids at 360−380 °C. After separation from the growth solution, the nanorods were dissolved in toluene. Subsequent gold growth onto the nanorods was performed by low-temperature reduction (273, 293, or 313 K) of $AuCl_3$ by varying amine ligands in the presence of dodecyldimethylammonium bromide (DDAB) with and without illumination by a 473 nm laser with 40 mW power. Further details of the syntheses are provided in the Supporting Information, along with details of the characterization techniques.

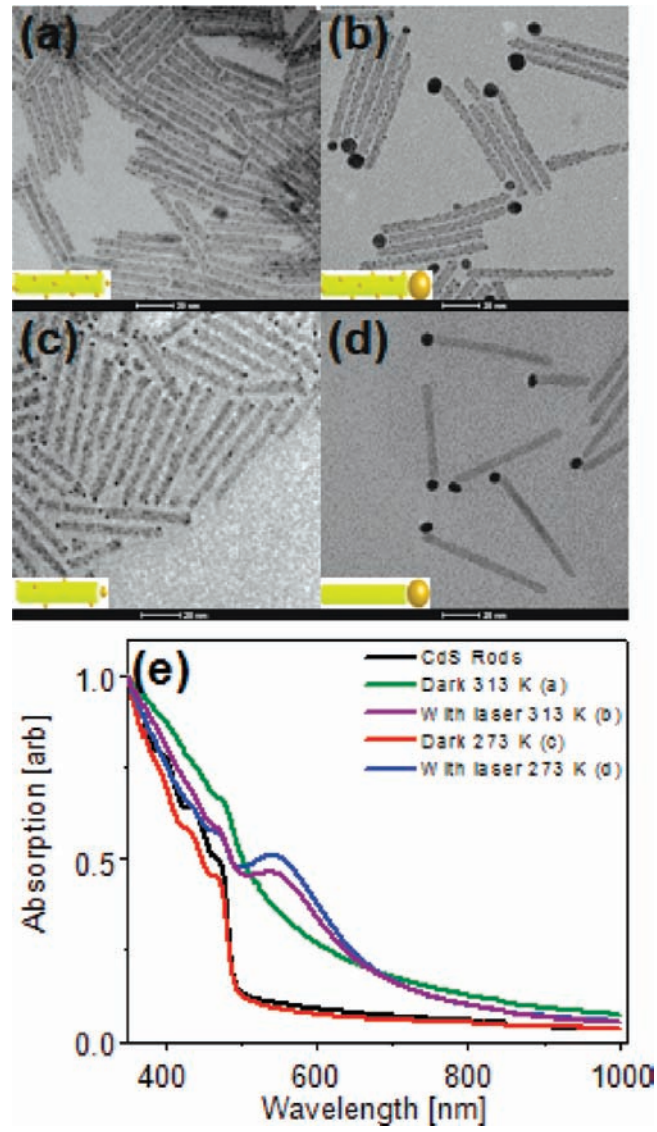

Figure 1. Au growth on CdS nanorods (58 × 5.1 nm) for 1 h: (a) dark at 313 K, (b) 473 nm laser irradiation at 313 K, (c) dark at 273 K, and (d) 473 nm laser irradiation at 273 K. The scale bar is 20 nm in all cases. (e) Normalized absorption spectra of CdS nanorods (black line) and the hybrid nanorods samples (colored lines).

Results and Discussion

Au was grown onto CdS nanorods (58 × 5.1 nm) under varying conditions, and the results are summarized in Figure 1. At 313 K and without illumination, we observed surface defect growth, as reported in an earlier study at room temperature (Figure 1a).[16] Illuminating the system at 473 nm under otherwise similar reaction conditions led to the growth of a large Au tip on one end of the rod ($d = 6 \pm 2$ nm), accompanied still by surface defect growth (Figure 1b). This indicates the presence of two reaction routes for Au growth: one occurring without light and leading to the defect growth, and another with light, leading to tip growth. The former was found to be strongly affected by temperature; defect growth was nearly suppressed at 273 K, usually with a small Au spot detected on one end of the rod (Figure 1c). The light-induced growth still took place at this reduced temperature (Figure 1d), thus achieving highly

(23) Subramanian, V.; Wolf, E. E.; Kamat, P. V. *J. Phys. Chem. B* **2003**, *107*, 7479–7485.
(24) Redmond, P. L.; Hallock, A. J.; Brus, L. E. *Nano Lett.* **2005**, *5*, 131–135.
(25) Dorfs, D.; Salant, A.; Popov, I.; Banin, U. *Small* **2008**, *4*, 1319–1323.
(26) Carbone, L.; Jakab, A.; Khalavka, Y.; Sönnichsen, C. *Nano Lett.* Published ASAP online Oct 8, 2009, http://dx.doi.org/10.1021/nl9017918.
(27) Hautman, J.; Klein, M. L. *J. Chem. Phys.* **1990**, *93*, 7483–7492.
(28) Wuister, S. F.; van Houselt, A.; Donega, C. D. M.; Vanmaekelbergh, D.; Meijerink, A. *Angew. Chem., Int. Ed.* **2004**, *43*, 3029–3033.
(29) Carbone, L.; et al. *Nano Lett.* **2007**, *7*, 2942–2950.

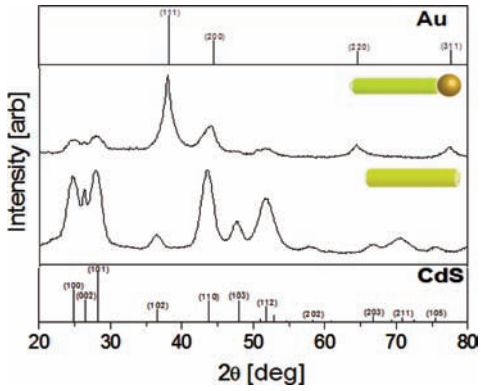

Figure 2. Powder X-ray diffraction pattern of a CdS nanorods sample before (bottom) and after (top) Au growth. The line patterns represent the expected position and intensity of the most intense XRD reflections for (bottom) bulk hexagonal (wurtzite) CdS and (top) fcc Au.

selective tip growth on one end ($d = 6.2 \pm 0.9$ nm) without defect growth. To ensure the versatility of this process, much longer CdS nanorods (120 × 6 nm) were tipped with gold in a similar manner, and little defect growth was observed (Figure S1, Supporting Information).

The differences in the hybrid structures grown under the various conditions are also clearly manifested in their absorption spectra (Figure 1e). Without light and at the higher temperature, only a small tail to the red of the CdS nanorod absorption was seen, accompanied by the broadening of the CdS nanorod excitonic features, which is consistent with defect growth.[16] With illumination, significant absorption of the Au plasmon was observed at about 540 nm, consistent with a large Au tip.[30] For growth at the lower temperature with illumination, the plasmon absorption was even more pronounced, with a clear peak at 540 nm, and the excitonic CdS peaks were maintained, indicating the high quality of the resultant hybrids.

Additional structural characterization of hybrids grown at 273 K under illumination is presented in Figure 2. The X-ray diffraction (XRD) pattern of the CdS nanorod templates showed the hexagonal wurtzite structure of CdS and matched well with the reflections observed for bulk CdS (Figure 2). In the hybrid, additional peaks indexed to face-centered cubic (fcc) Au were present and were significantly stronger than the CdS peaks because of the large tip size and the strong Au X-ray scattering factor.[31]

The crystallinity of the hybrid structures was also revealed in the high-resolution transmission electron microscopy (HRTEM) images (Figure 3), which showed either CdS or Au lattice fringes on the respective segments of the hybrid. In Figure 3, we indexed these lattice fringes on the basis of the measured *d*-spacing values. As expected, (002)-type fringes perpendicular to the growth direction of hexagonal close-packed (hcp) CdS nanorods were seen in the semiconductor segments of the hybrids, while in the Au tips we observed fringes corresponding to (111) and (200)-type atomic planes of fcc Au. In many cases, nanocrystalline gold tips appeared as twinned or multiply twinned particles.[32,33] The relative positioning of the large Au tip varies in the different particles, showing straight growth on the apex (Figure 3a,b) or growth at an angle (Figure 3c). Such varying positioning for the Au tip growth is assigned to the facet topology at the end of the nanorod, as previously analyzed by Ryan and co-workers for vertical arrays of nanorods.[34] In some hybrids, an elongated Au particle was also observed (Figure 3b).

We next turned to analyze the mechanism responsible for the defect growth, which was strongly influenced by temperature, clearly indicating a thermally activated kinetic effect. To this end, we carried out Au growth experiments under illumination in the presence of several different amine ligands (Figure 4). These experiments were carried out on seeded CdSe/CdS nanorods (CdSe seed size 2.9 nm, with a thick CdS shell of 1.2 nm, rod dimensions 56 × 5.3 nm) to demonstrate the generality of the growth approach to other related heterostructured rods. Although defect growth could be suppressed by reducing the growth temperature from 293 to 273 K in the presence of dodecylamine (DDA) (Figure 4a,b), when instead a longer alkylamine, octadecylamine (ODA), was used, defect growth was fully suppressed even at the higher temperature (293 K, Figure 4c). On the other hand, trioctylamine (TOA), a much bulkier ligand than DDA, yielded pronounced defect growth even at low temperature (273 K, Figure 4d). Indeed, the quality of the absorption of the gold plasmon of these products also indicated temperature- and ligand-dependent growth behavior (Figure S2, Supporting Information). This is consistent with a previous reports on the photodeposition of Pt on CdS nanorods at high temperatures, where only tertiary amines yielded growth of small Pt dots on the rod sides, while primary amines led to little deposition.[22] The combination of ligand exchange and temperature effects modifying the rate of growth on surface defects points to the important role of the passivating surface layer with regard to the growth of the metal on rod defects.

Previously, the influence of capping alkyl amines of various lengths on the temperature dependence of fluorescence of CdSe QDs was studied. Higher temperatures gave stronger emissions. This behavior was assigned to a phase transition of the alkyl chains, which at higher temperatures are more dynamic, allowing for better passivation of surface traps. This phase transition was found to depend on the alkyl chain length, where longer chains manifest a higher transition temperature. DDA (C12) at 273 K already reached the dynamic phase, while ODA (C18) reached this state only at ~305 K.[28] This behavior is fully consistent with our observations of the effects of temperature and ligand identity on the gold defect growth on CdS nanorods studied here. Defect growth is seen when the ligands are in the higher temperature phase; the ligand mobility allows the gold precursor to access the rod surface more readily. Defect growth is blocked at the low temperature when the ligands are in the static phase, sterically blocking access of the gold to the rod surface. The longer chain ligands provide static passivation, even at higher temperature, because they remain in their static state. Control reactions without amine ligands showed aggregation of the nanocrystals, with a small amount of Au growth observed on defects and at the seed position at both 273 and 293 K (Figure S3, Supporting Information). This result confirms that both the use of amine ligands and illumination of the samples are needed for selective Au tip growth.

(30) Alvarez, M. M.; Khoury, J. T.; Schaaff, T. G.; Shafigullin, M. N.; Vezmar, I.; Whetten, R. L. *J. Phys. Chem. B* **1997**, *101*, 3706–3712.
(31) Lonsdale, K. *International Tables for X-Ray Crystallography*; The International Union of Crystallography: Birmingham, 1962; Vol. 3, pp 202, 211−212.
(32) Hofmeister, H.; Dubiel, M.; Tan, G. L.; Schicke, K. D. *Phys. Status Solidi A* **2005**, *202*, 2321–2329.
(33) Ino, S. *J. Phys. Soc. Jpn.* **1969**, *27*, 941–953.
(34) O'Sullivan, C.; Ahmed, S.; Ryan, K. M. *J. Mater. Chem.* **2008**, *18*, 5218–5222.

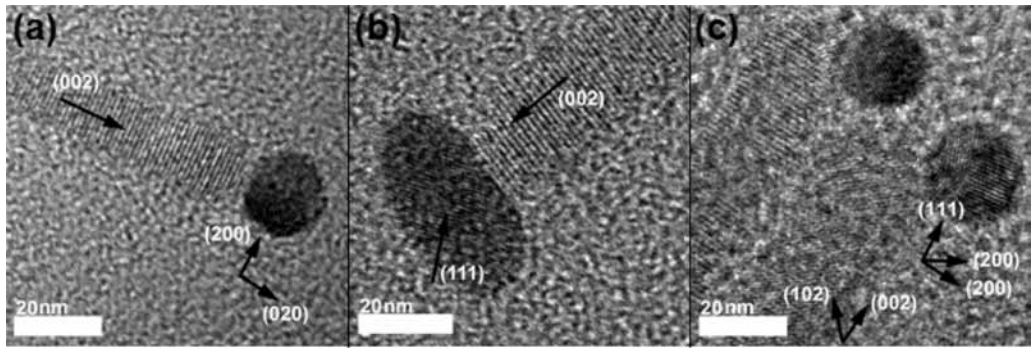

Figure 3. HRTEM measurements of CdS−Au hybrids, showing the relative positioning of the large Au tip in different nanorods. Visible lattice fringes within CdS and Au crystalline segments of the hybrids are indexed according to the as-measured *d*-spacing values (0.335 and 0.245 nm for (002) and (102) CdS, respectively; 0.235 and 0.203 nm for (111) and (200) Au, respectively). Black arrows indicate normals to the indexed lattice planes.

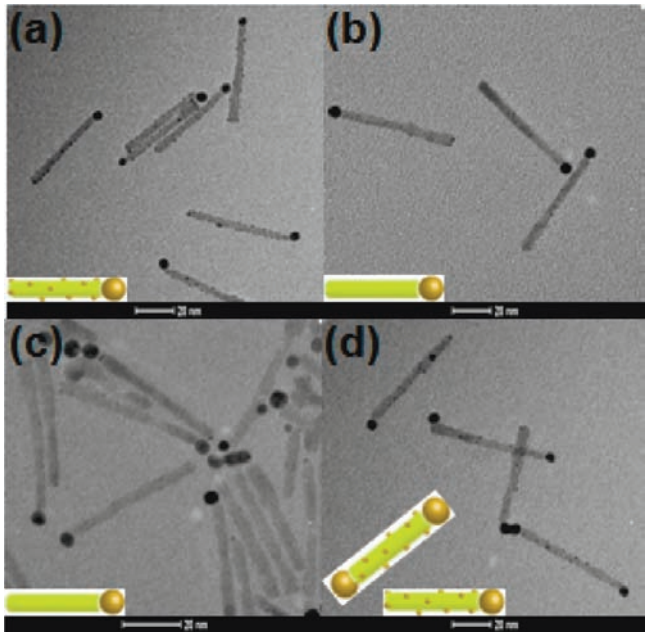

Figure 4. Au growth on seeded CdSe/CdS nanorods (56 × 5.3 nm) after 30 min of 473 nm laser irradiation with different temperatures and ligands: (a) 293 K and DDA, (b) 273 K and DDA, (c) 293 K and ODA, and (d) 273 K and TOA. The scale bar is 20 nm in all cases.

Our results and interpretation also agree with the calculations by Vlugt and co-workers on the temperature-dependent absorption of a hexylamine capping layer onto a similar system of CdSe dots.[35] According to their calculated adsorption isotherms, the number of adsorbed ligands decreases with increasing temperature. When gold growth was performed at a lower temperature, more ligands were adsorbed to the CdS nanorod, passivating the surface, and therefore defect growth was prevented.

Seeded rods were employed to further investigate the location of the deposited Au tips and the reason by which growth of one tip is dominant. The seed location was used as a marker for the anisotropic growth process. Previous structural studies showed that the seed was located about one-fourth of the way from the slow-growing, Cd-rich end of the rod,[29] as was corroborated by the Au location upon deposition in dark conditions (Figure 6a).[17]

This study was carried out on seeded CdSe/CdS nanorods (CdSe seed size 3.9 nm, thick CdS shell of 2 nm, rod dimensions 28 × 8 nm) with large CdSe seeds to aid in identification of the seed position. Slightly bullet-shaped particles were chosen rather than rods to also help elucidate the anisotopic growth of the gold.[36−39] Since TEM imaging did not show a contrast difference between the CdS rod and CdSe seed (Figure 5a inset), we turned to elemental-sensitive analytical techniques. The highly Z-sensitive imaging method of high angular annular dark-field scanning transmission electron microscopy (HAADF-STEM) easily contrasted the Au and CdSe/CdS regions (Figure 5a) but still was not sensitive enough to identify the CdSe seed position. Figure 5b presents energy dispersive X-ray spectroscopy (EDS) line scans acquired in STEM mode on bullet-shaped rods. The Au and Se signals were followed, with the inset STEM image showing the line along which each scan was taken. In Figure 5b,c we observed a Au peak close to one end and a weak Se peak (due to the small amount of Se in the seed) near the other end of the nanorod. The straight growth on the apex and the position of the gold compared to the seed can be rationalized considering that the fast-growing $(00\bar{1})$ facet of the rod is sulfur-rich, with likely many negative dangling bonds.[37,40,41] These surfaces would therefore actively and effectively initiate nucleation from the sulfophilic and cationic gold precursor to form Au−S bonds, which have very high bond enthalpies (a diatomic bond enthalpy of 418 kJ/mol), promoting this growth.[42] Furthermore, this facet may have better transport of gold cations to it, as the amine ligands likely bond less strongly to the negatively polarized, sulfur-rich surface than to the more positive, cadmium-containing ones.[37,40,41]

Figure 5c shows growth at the same end relative to the seed but at an angle. In this case the growth occurred onto a $(10\bar{1})$ facet; these facets are also sulfur-rich when excess TOP−calcogenide is used in the synthesis,[43,44] as is the case here.

Figure 5d shows another rod in which the Au and Se peaks are near the same end. In this case, the gold tip is seen to grow at an angle to the rod axis, consistent with growth onto a (101)

(35) Schapotschnikow, P.; Hommersom, B.; Vlugt, T. J. H. *J. Phys. Chem. C* **2009**, *113*, 12690–12698.

(36) Jun, Y. W.; Casula, M. F.; Sim, J. H.; Kim, S. Y.; Cheon, J.; Alivisatos, A. P. *J. Am. Chem. Soc.* **2003**, *125*, 15981–15985.
(37) McBride, J.; Treadway, J.; Feldman, L. C.; Pennycook, S. J.; Rosenthal, S. J. *Nano Lett.* **2006**, *6*, 1496–1501.
(38) Nair, P. S.; Fritz, K. P.; Scholes, G. D. *Small* **2007**, *3*, 481–487.
(39) Scholes, G. D. *Adv. Funct. Mater.* **2008**, *18*, 1157–1172.
(40) Peng, Z. A.; Peng, X. G. *J. Am. Chem. Soc.* **2001**, *123*, 1389–1395.
(41) Puzder, A.; Williamson, A. J.; Zaitseva, N.; Galli, G.; Manna, L.; Alivisatos, A. P. *Nano Lett.* **2004**, *4*, 2361–2365.
(42) Lide, D. R. *CRC Handbook of Chemistry and Physics*, 81st ed.; CRC: Boca Raton, FL, 2000; pp 9−52.
(43) Taylor, J.; Kippeny, T.; Rosenthal, S. J. *J. Cluster Sci.* **2001**, *12*, 571–582.
(44) Jasieniak, J.; Mulvaney, P. *J. Am. Chem. Soc.* **2007**, *129*, 2841–2848.

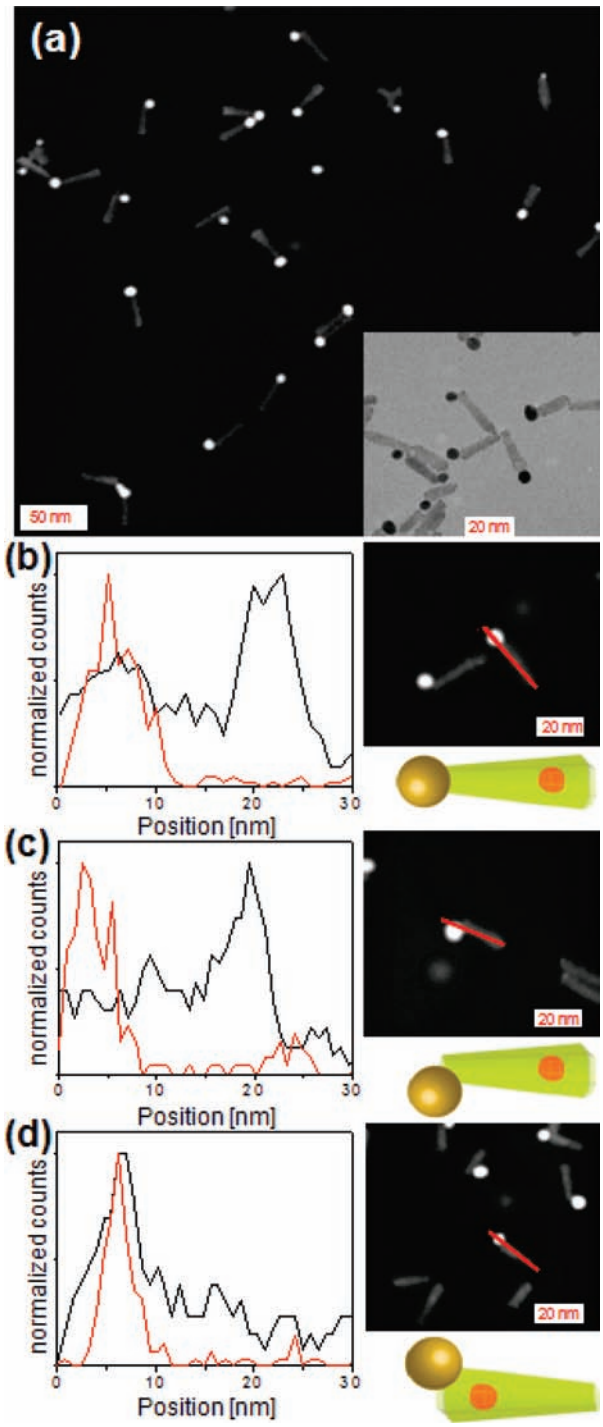

Figure 5. (a) HAADF-STEM image of seeded CdSe/CdS nanorods (28 × 8 nm) with gold growth onto them; inset shows TEM image of the same sample. (b) Elemental analysis (EDS line scan, 1.0 nm step size; red line Au, black line Se) of a single nanorod with Au growth on the apex that is located far from the seed position. (c) EDS line scan of a single nanorod with a gold tip grown at an angle and located opposite to the seed position. (d) EDS line scan of a single nanorod with a gold tip grown at an angle and close to the seed position. The selenium signal is weak due to low amounts of the element in the seed and was smoothed by the running average method.

facet (located near the flat and wider end of the rod), and although it is on the slow-growing end of the rod, this particular facet is also sulfur-rich.[37]

One intriguing aspect of the growth onto sulfur-rich facets relates to the selective deposition on only one end of the rod

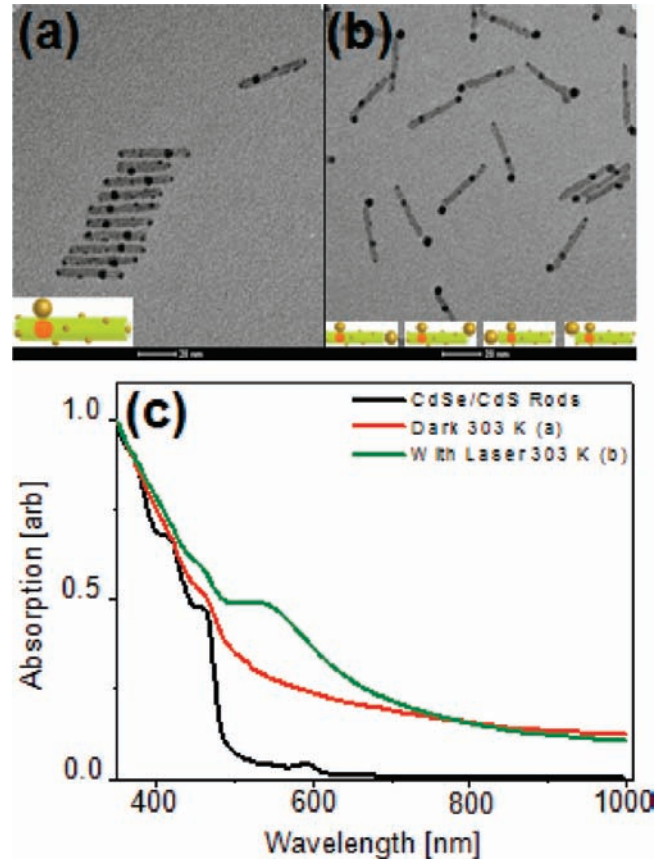

Figure 6. Au growth on seeded CdSe/CdS nanorods (37 × 4.9 nm) for 1 h at different conditions with ODA ligands: (a) under dark conditions at 303 K, and (b) with 473 nm laser irradiation at 303 K. The scale bar is 20 nm in both cases. (c) Normalized absorption spectra of the seeded nanorods and the different samples.

under illumination. Once a gold island nucleates on one end, that initial island facilitates light-induced charge separation between the metal and semiconductor segments[9,10,15] and serves as a sink for the electrons of the excited electron−hole pairs. The now negatively charged island facilitates the reduction of additional gold precursor (the holes are concomitantly transferred to the amines), leading to further growth on that initial seed. This explains the observed asymmetric growth behavior.

We previously reported selective metal deposition without illumination onto the seed location for CdSe/CdS heterostructures with thin CdS shells.[17] We therefore investigated the competition between Au growth via a thermal route and light-induced growth on such structures. Figure 6 shows TEM images for Au growth under varying conditions on seeded CdSe/CdS nanorods (CdSe seed 3.4 nm, with a thin CdS shell of 0.7 nm, rod dimensions 37 × 4.9 nm), using ODA as the amine at $T =$ 313 K. Without laser irradiation, we observed selective growth of a large Au island ($d = 3.8 \pm 0.6$ nm) at the seed location, along with defect growth of smaller Au islands along the rod body (Figure 6a), consistent with our previous report.[17]

Irradiating the sample with 473 nm laser at this higher temperature resulted in growth of two large gold particles, one at the apex ($d = 4.5 \pm 0.9$ nm) and the second smaller one at the seed location ($d = 3.0 \pm 0.6$ nm) (Figure 6b). This is accompanied by a clear Au plasmonic absorption peak at 530 nm as a result of a large Au tip on the end (Figure 6c).[30] For these seeded rods with a thin shell, thermal growth is electro-

chemical Ostwald ripening,[24] leading to selective deposition at the seed location. Once illumination is added, the thermal growth is somewhat diminished by tip growth; therefore, the size of the gold spot at the seed location decreases.

In order to gain further understating of the factors determining the position of the gold tip, the position of the tip relative to the gold spot at the seed location was noted for 200 particles (Figure 6b). A total of 35% of the particles have a gold tip that is located far from the seed position and show a straight growth on the apex. An additional 35% of the particles have a gold tip that is located far from the seed position, but growth is at an angle. Another 22% of the particles have a gold tip that is located close to the seed position with growth at an angle. For these three cases we assign the growth onto the sulfur-rich facets, the $(00\bar{1})$, $(10\bar{1})$, and (101), respectively.[37,43,44] The remaining gold tips (8%) grow at the end close to the seed position but show a straight growth on the apex. The CdS surface is known to be chemically etched by DDAB.[1] Therefore, we attribute this growth to exposure of the sulfur as a result of etching during the reaction of an originally cadmium-rich (001) facet.[37] This kind of tip growth is less abundant since the etching occurs at a slow rate, giving priority to growth on the other facets mentioned above.

Conclusions

Two competing mechanisms were identified for Au growth onto CdS-based nanorods. The thermal route leads to defect growth which can be suppressed at lower temperatures, while light-induced growth leads to selective deposition on one end of the rods. The temperature dependence was attributed to the phase transition of the ligand alkyl chains, blocking effective access of Au precursor to the surface at lower temperatures. This was corroborated by the ligand effect, where longer chain amines provided improved blocking of surface defect growth, even at room temperature. The tip was shown to grow on sulfur-rich facets of the nanorod, producing end-on and angled tip orientations. The controlled formation of the anisotropic structure of Au-tipped CdS nanorods enriches the selection of building blocks for devices and applications that could exploit the anistropy of the system.

Acknowledgment. We thank Dr. Haviv Grisaru from the Unit for Nanocharacterization for technical assitance and Amit Sitt for helpful discussions. The work was supported in part by the NanoSci ERANET program (project Single Nanohybrid). U.B. acknowledges support from the Alfred and Erica Larisch Memorial Chair in Solar Energy.

Supporting Information Available: Experimental procedures, additional TEM characterization, optical data, and complete ref 29. This material is available free of charge via the Internet at http://pubs.acs.org.

JA9077733